



LAWRENCE
LIVERMORE
NATIONAL
LABORATORY

X-ray Laser Interferometry of Confined Laser-Produced plasmas

J. Dunn, S. J. Moon, J. Nilsen, M. Purvis, J. Filevich, J.
Grava, M. C. Marconi, J. J. Rocca, V. N. Shlyaptsev

February 5, 2010

X-ray Lasers 2008
Belfast, United Kingdom
August 17, 2008 through August 22, 2008

Disclaimer

This document was prepared as an account of work sponsored by an agency of the United States government. Neither the United States government nor Lawrence Livermore National Security, LLC, nor any of their employees makes any warranty, expressed or implied, or assumes any legal liability or responsibility for the accuracy, completeness, or usefulness of any information, apparatus, product, or process disclosed, or represents that its use would not infringe privately owned rights. Reference herein to any specific commercial product, process, or service by trade name, trademark, manufacturer, or otherwise does not necessarily constitute or imply its endorsement, recommendation, or favoring by the United States government or Lawrence Livermore National Security, LLC. The views and opinions of authors expressed herein do not necessarily state or reflect those of the United States government or Lawrence Livermore National Security, LLC, and shall not be used for advertising or product endorsement purposes.

X-ray Laser Interferometry of Confined Laser-Produced plasmas

J. Dunn ^{a)}, S.J. Moon, and J. Nilsen

Lawrence Livermore National Laboratory, Livermore, CA 94551

M. Purvis, J. Filevich, J. Grava, M.C. Marconi, and J.J. Rocca

***NSF ERC for Extreme Ultraviolet Science and Technology and Dept. of Electrical and
Computer Engineering, Colorado State University, Fort Collins, CO 80523***

V. N. Shlyaptsev

University of California Davis-Livermore, Livermore, CA 94551



**Presented at the International Conference on X-ray Lasers,
Belfast, Northern Ireland, August 17 - 22, 2008**

LLNL-CONF-423238

^{a)} dunn6@llnl.gov

This work performed under the auspices of the U.S. Department of Energy by Lawrence Livermore National Laboratory under Contract DE-AC52-07NA27344, through the Institute of Laser Science and Applications and in part sponsored by the National Nuclear Security Administration under the Stewardship Science Academic Alliances program through U.S. Department of Energy Research Grant #DE-FG52-06NA26152.

Outline



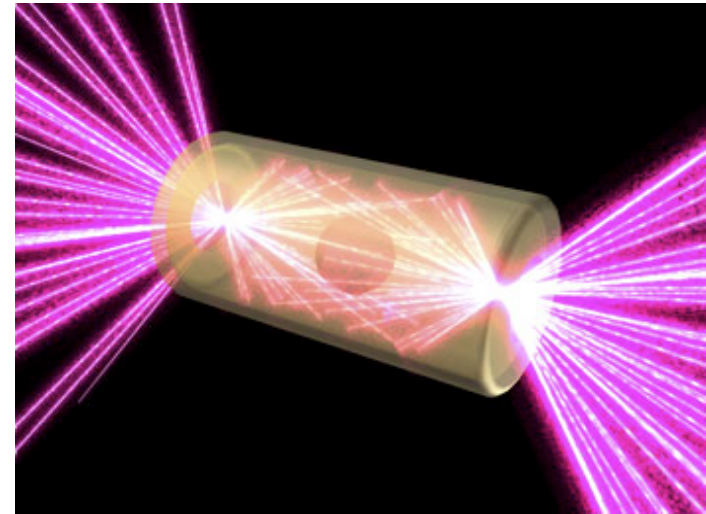
- **Motivation**
- **Benefits of short wavelength probes for measuring plasmas**
- **X-ray laser interferometry setup**
- **Target geometry:**
 - I. Planar Targets comparison with 2-D LASNEX
 - II. Deep rectangular groove target experiments
 - III. 3-Dimensional (3-D) hydrodynamic simulation code HYDRA
 - IV. Semi-cylindrical targets comparisons with HYDRA
 - V. V-groove targets comparisons with HYDRA
- **Summary**

Motivation: Improve understanding of physics in dense plasmas with ultra-bright soft x-ray laser interferometry



Determine physical processes:

- Laser-heated plasmas (and other)
- Ablation
- Energy deposition and (non-)local heating
- Production of converging plasmas
- Formation of plasma jets
- Provide precise experimental data sets for benchmarking codes
- ICF hohlraums including NIF
- Shock unloading of surfaces
- Relevant to astrophysical plasmas



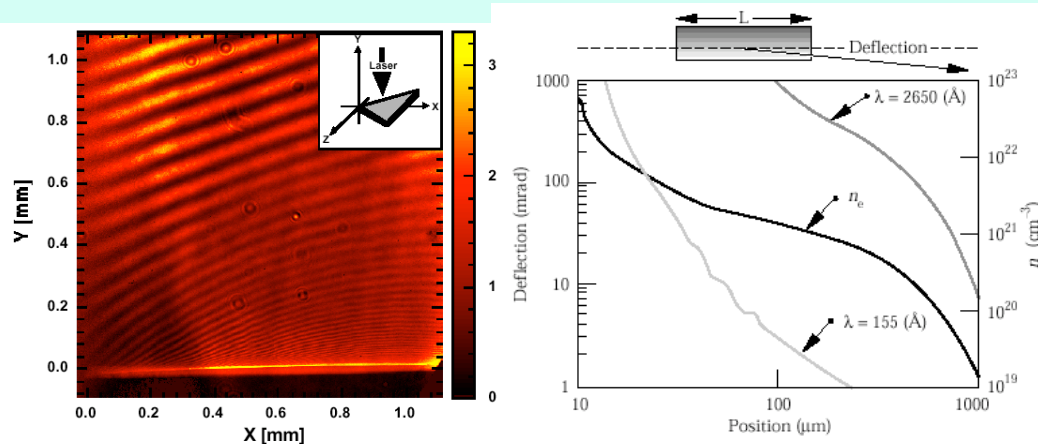
Artist 3D rendering of a NIF hohlraum
(www.llnl.gov/nif)

**NIF construction stage
completed in 2009 Q1,
National Ignition Campaign
begins**

**Greater understanding of energy transport mechanisms in LPP in
order to check physics in hydrodynamic codes**

Reduced refraction and absorption are main benefits of XRL interferometry over optical and UV beams

X-ray probes are deflected substantially less in plasma density gradients: probe higher density plasmas



Da Silva *et al*, PRL **74**, 3991 (1995).

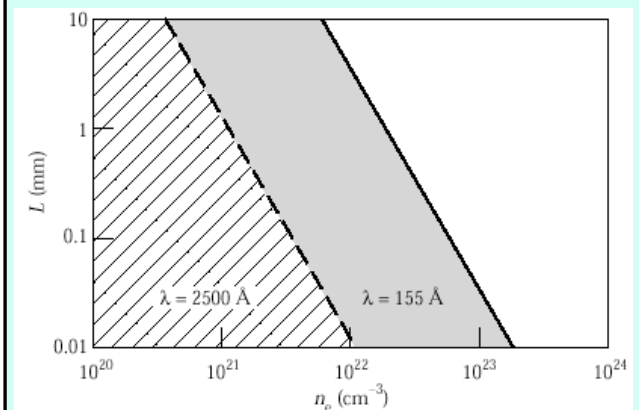
For linear density gradient:

$$n_e = n_o [1 - (y/y_o)]$$

Deflection angle scales as:

$$\theta \propto \lambda^2 L / y_o$$

Larger parameter space accessible to 15.5 nm x-ray laser



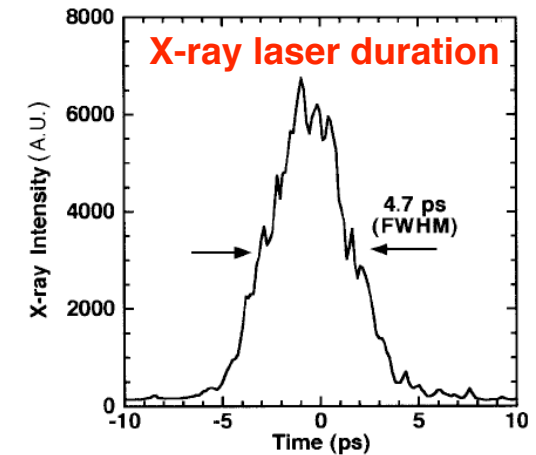
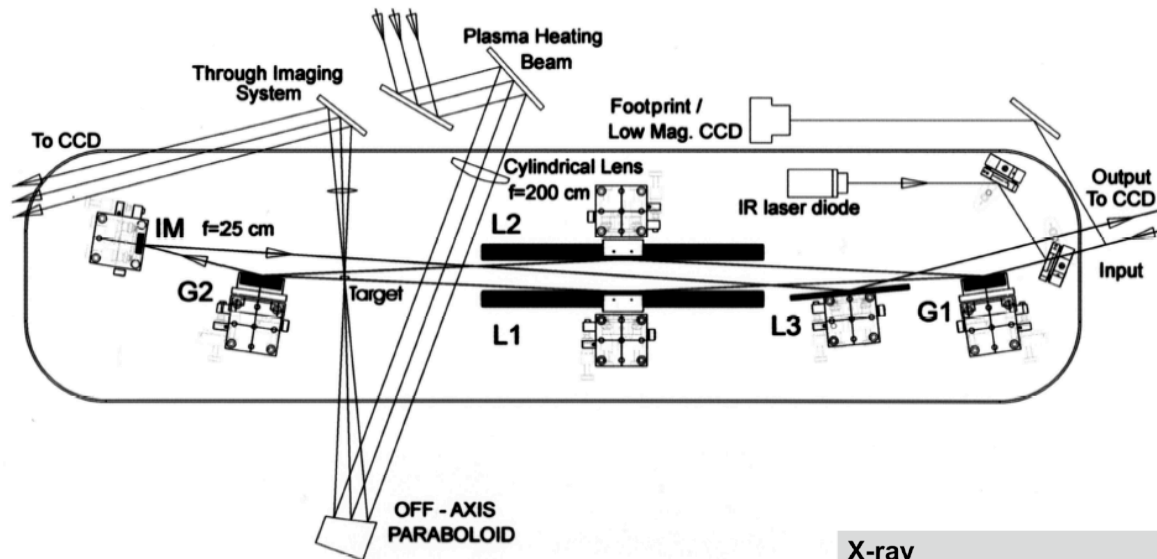
- Only bremsstrahlung absorption considered

$$\alpha = 2.42 \times 10^{-37} \frac{\langle Z^2 \rangle n_e n_i}{\sqrt{T_e} (h\nu)^3} [1 - \exp(-h\nu / kT_e)]$$

- Abs. scales as $h\nu^{-2}$ if $h\nu \ll kT_e$

**Other benefits include reduced number of fringes can be resolved $\sim \lambda$
Recent tabletop x-ray lasers have improved ps time resolution, faster shot rate giving improved measurements to test simulation database**

X-ray Laser Interferometry with grating beam splitters first demonstrated at 46.9 nm at CSU, extended to 14.7 nm



Notes:

Amplitude division interferometer based on skewed Mach-Zehnder geometry

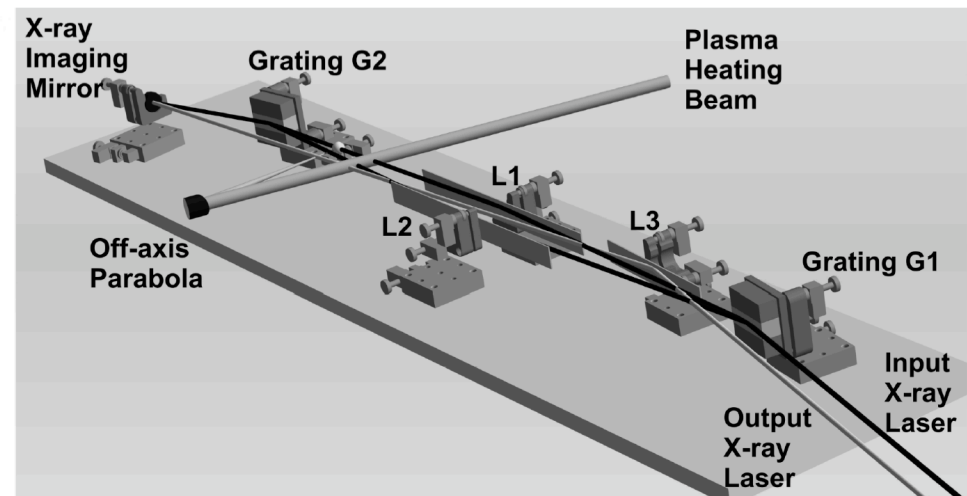
Interferometer uses 0th and 1st orders

G1, G2 beam splitters: 900 l/mm

X-ray Imaging optic: Mo:Si coated $f = 25$ cm spherical mirror

Magnification: 22 x

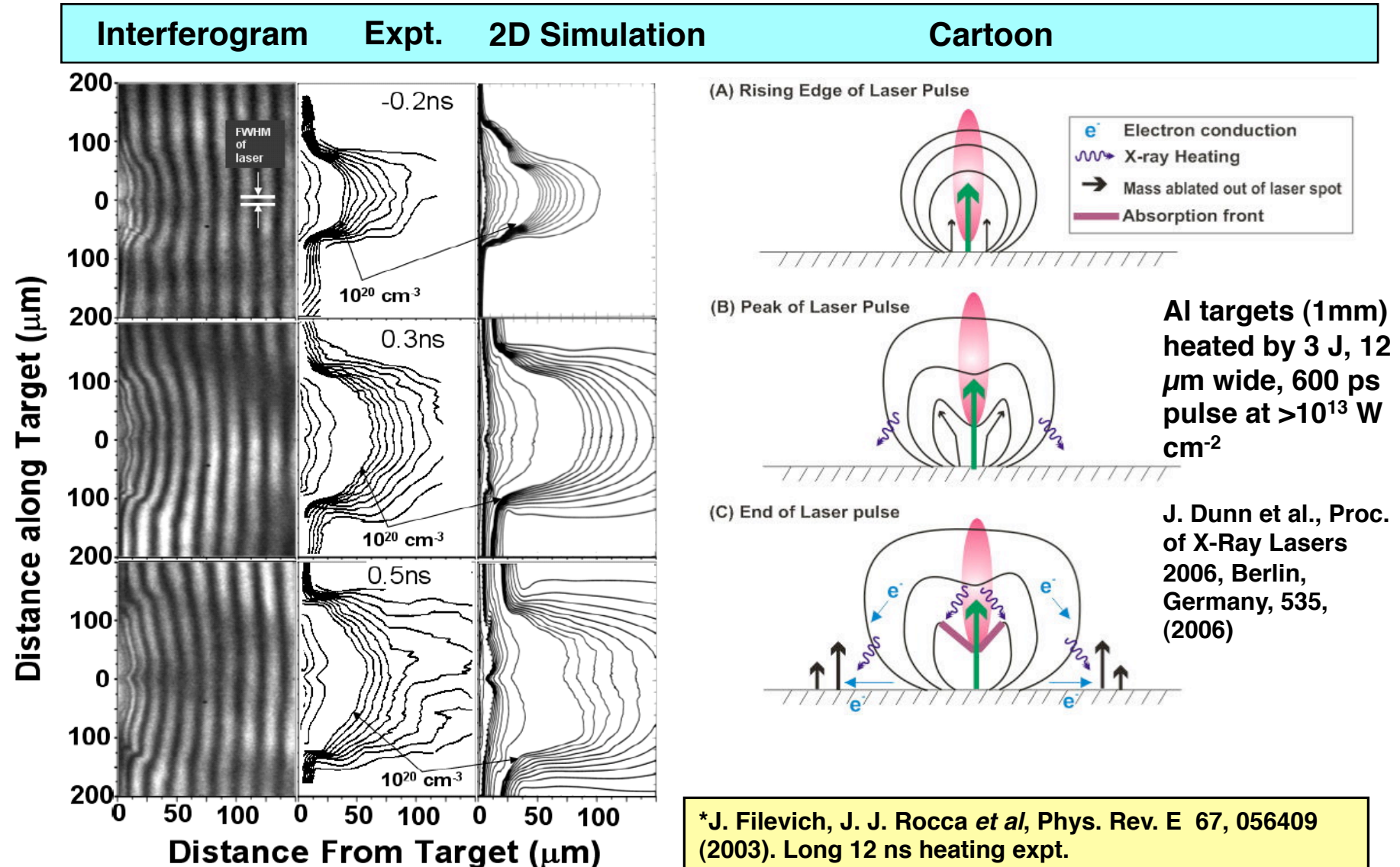
Back-thinned CCD detector: 0.5 μm spatial resolution



J. Filevich, K. Kanizay, M. C. Marconi, J. L. A. Chilla, and J. J. Rocca, *Optics Letters* 25, 356 (2000).

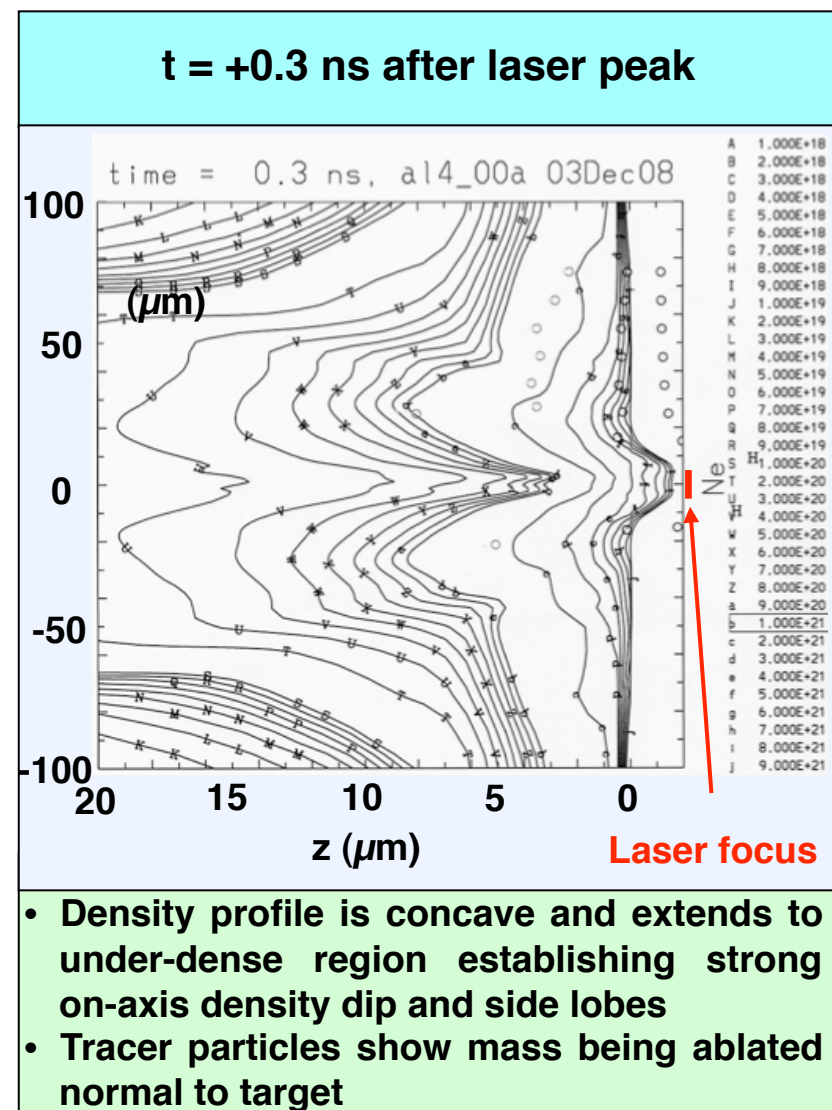
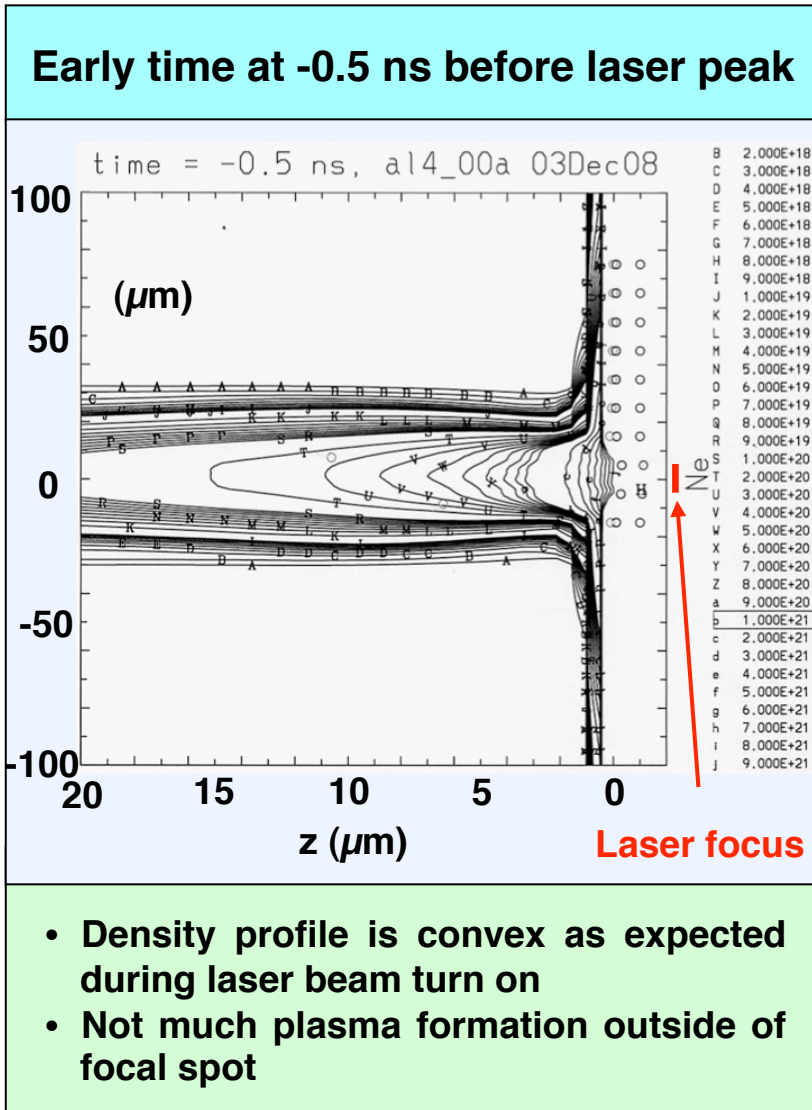
J. Filevich *et al.*, *Appl Opt.* 43, 3938 (2004).

I. Planar targets: Data compared with 2D LASNEX on-axis show density dip, energy deposition outside of focus



On axis dip, formation of side lobes also observed previously*

LASNEX shows as plasma evolves during laser pulse, lateral transport generates heated plasma outside of focus

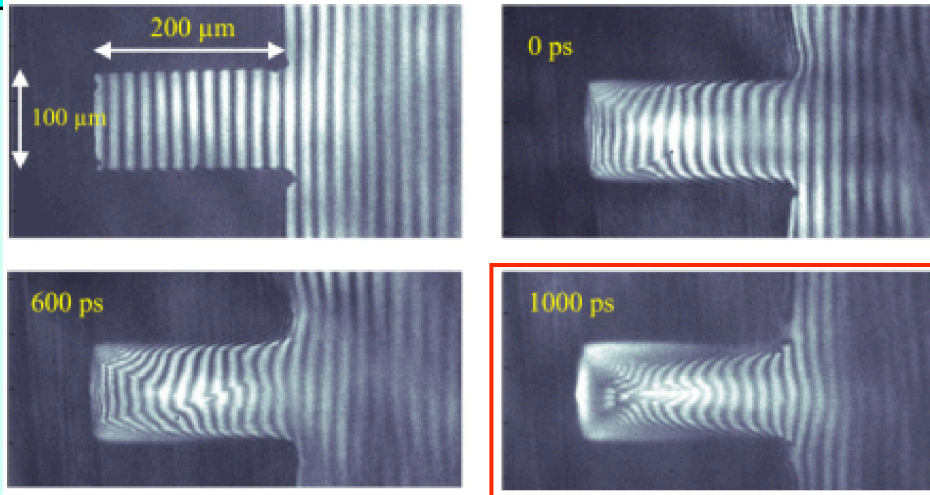


***Above simulations are generated using square spatial profile with no spatial wings and actual laser temporal pulse shape**

II. Deep rectangular groove: Laser-heated confined target geometry gives insight into colliding plasmas



Al groove heated by 600 ps, 10^{13} W cm $^{-2}$ laser tightly focused to 12 μ m

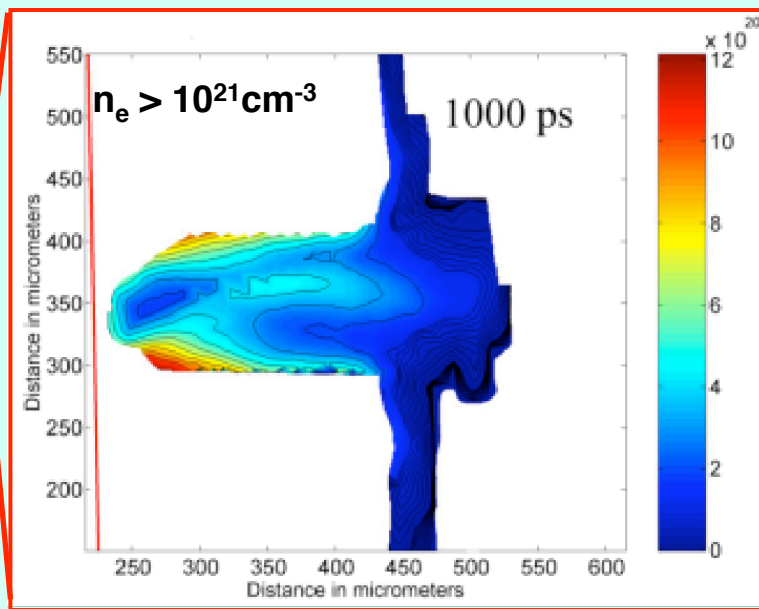


Groove: 100 μ m x 200 μ m x 1mm (W x D x L)

15 temporal snapshots for -0.3 ns to 3 ns

Times relative to peak of 600 ps heating pulse

Density map of Al groove



Observe evolution of many interesting plasma phenomena

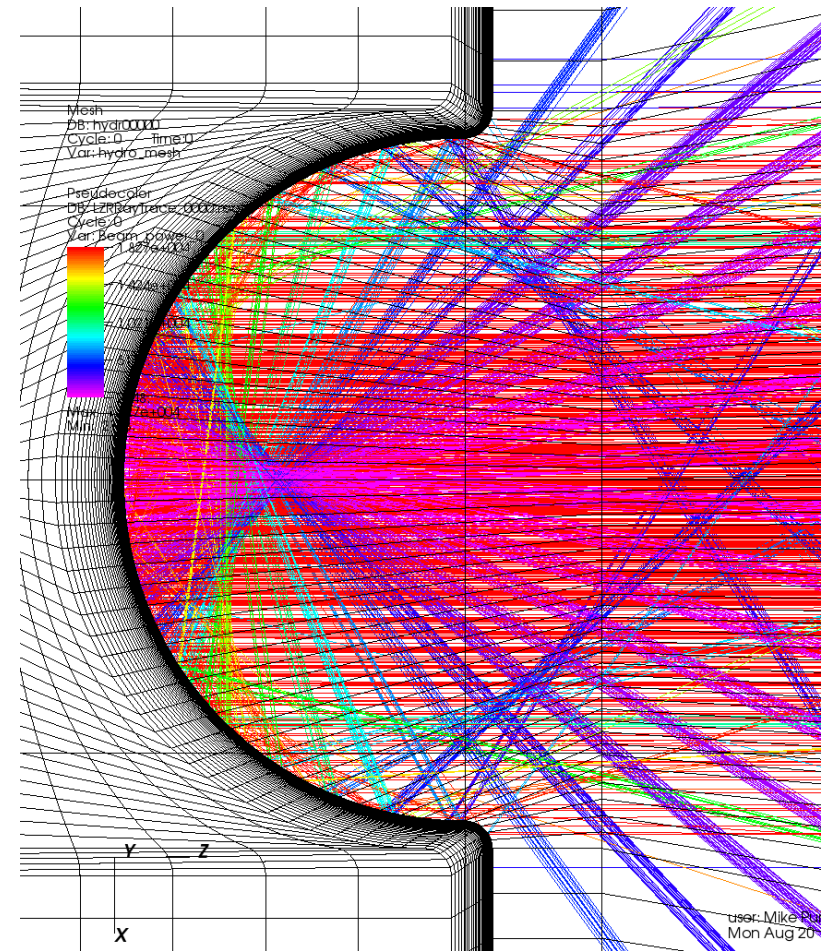
- Confined expansion
- Heating in corners
- Formation of multiple jets
- Colliding plasma
- On-axis depression
- Cold material from walls radiatively heated at later times

III. 3-Dimensional (3-D) code HYDRA developed for ICF used to model semi-cylindrical and V-groove targets



- Developed at Lawrence Livermore National Labs
- Our simulations performed in 2D
 - Structured mesh made up of hexahedrons.
 - Lagrangian --> Arbitrary Lagrangian Eulerian (ALE).
 - Mesh adaptively follows plasma.
- Single fluid: $n_e = Z \cdot n_i$.
- 3 temperatures: T_e , T_i , T_{rad} .
- Radiation transport
 - Multi-group
 - Tabulated opacities from LLNL's LEOS library
- Laser ray trace
 - Random spatial and energy distributions.
 - Included heating from reflected rays.
 - Inverse Bremsstrahlung absorption.
- Heat conduction
 - Conductivities of Lee and More
- E.O.S. from LLNL's LEOS library
- Thomas-Fermi model for ionization

M.M. Marinak, S.W. Haan, T.R. Dittrich, R.E. Tipton, and G.B. Zimmerman, *Physics of Plasmas*, 5(4), 1125 (1998).

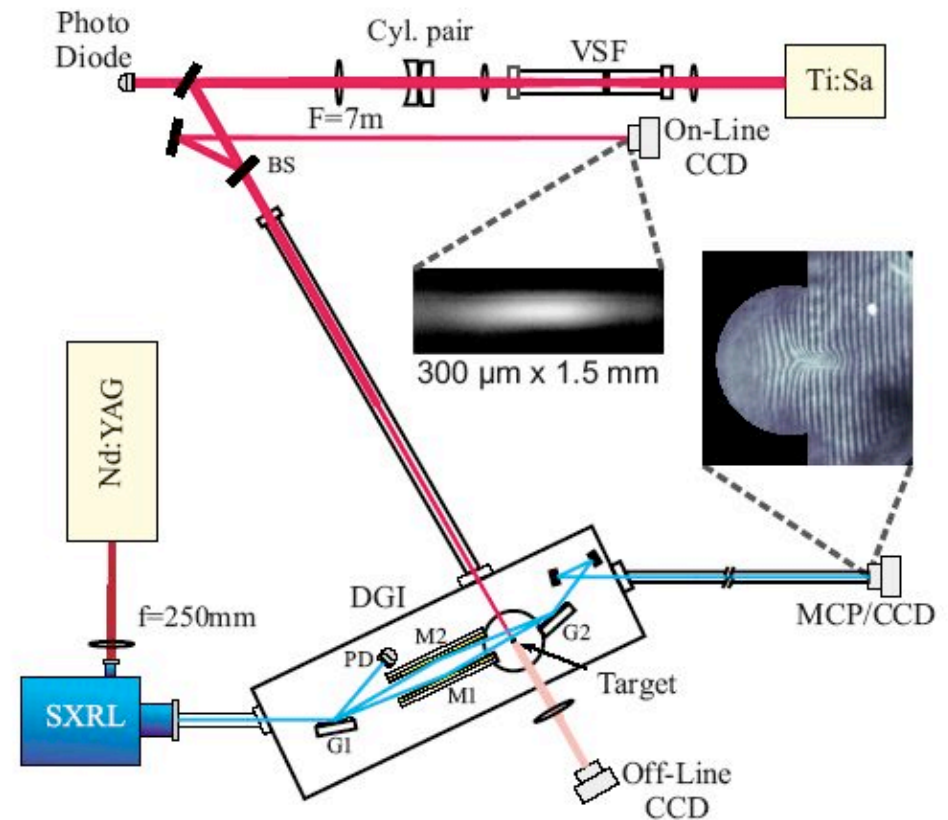
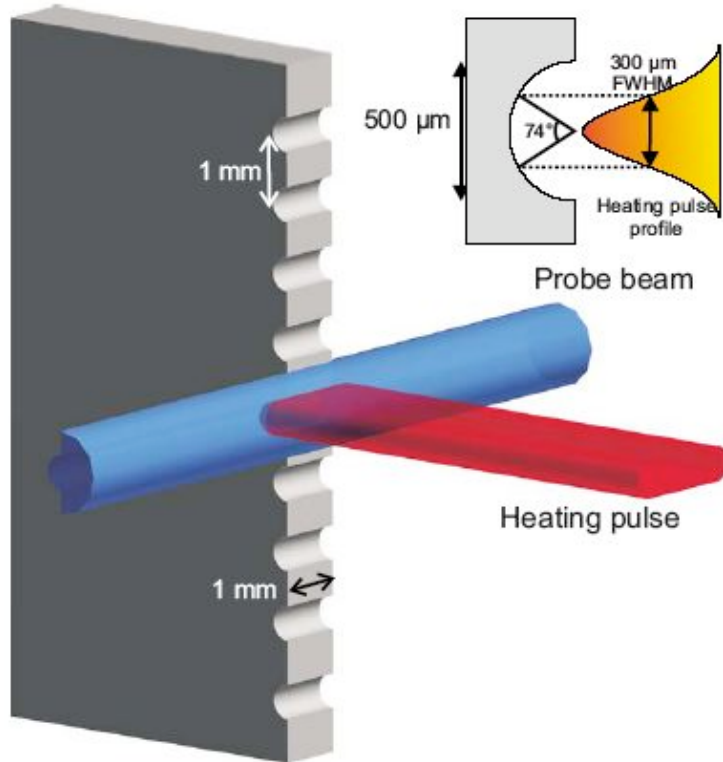


Time = 0 Grid/Ray trace visualization

IV. Semi-cylindrical target: Experimental setup at CSU for probing laser-heated half-hohlraum type geometry

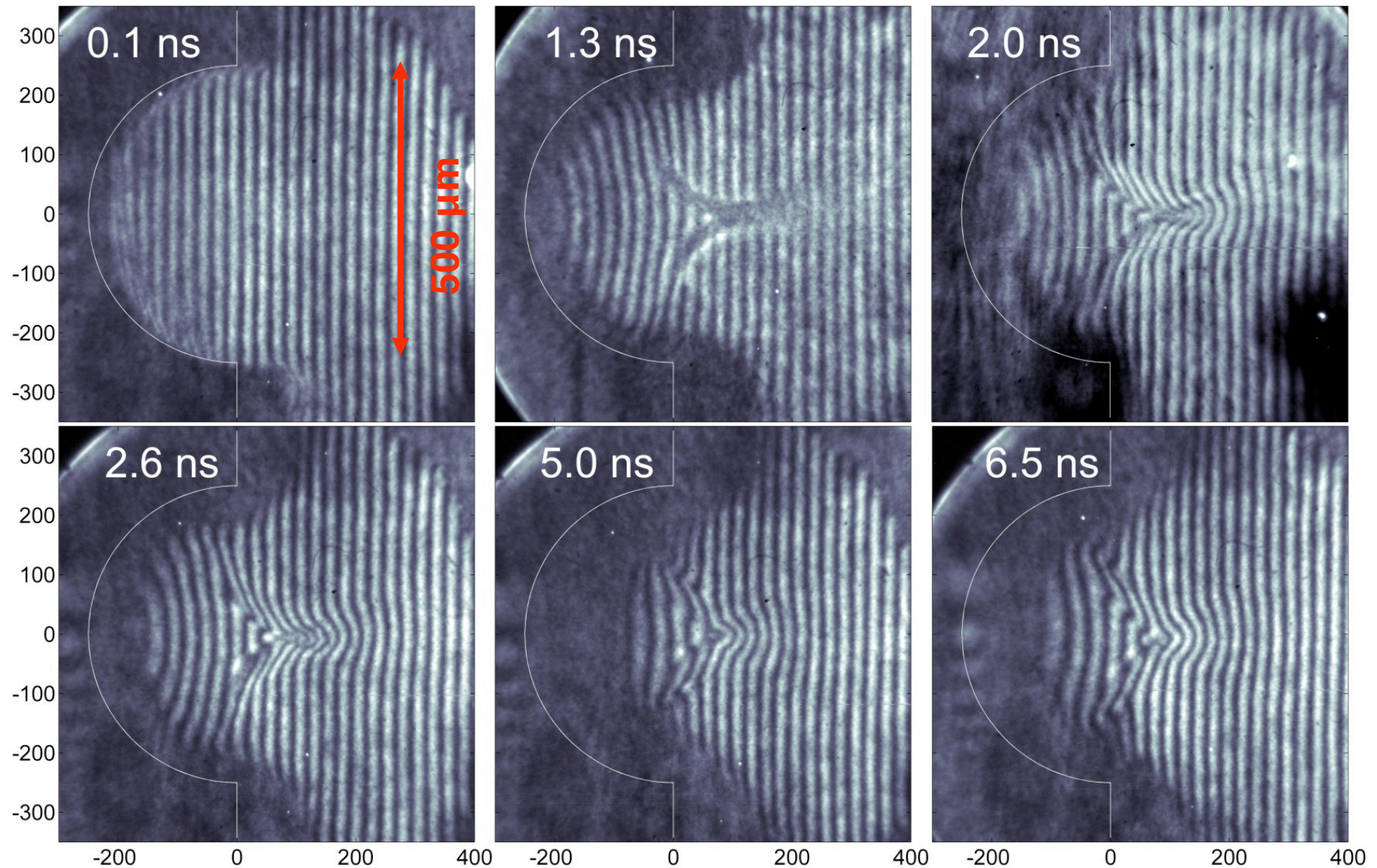
Laser Irradiation conditions:

- 10^{12} Wcm^{-2} , 600 mJ at 800 nm wavelength, 120 ps (FWHM)
- Laser focus: $300\mu\text{m} \times 1.5\text{mm}$ line



M. Purvis, J. Grava, J. Filevich, M. C. Marconi, J. J. Rocca, J. Dunn, S. J. Moon, V. N. Shyaptsev, E. Jankowska", Phys. Rev. E 76, 046402 (2007)

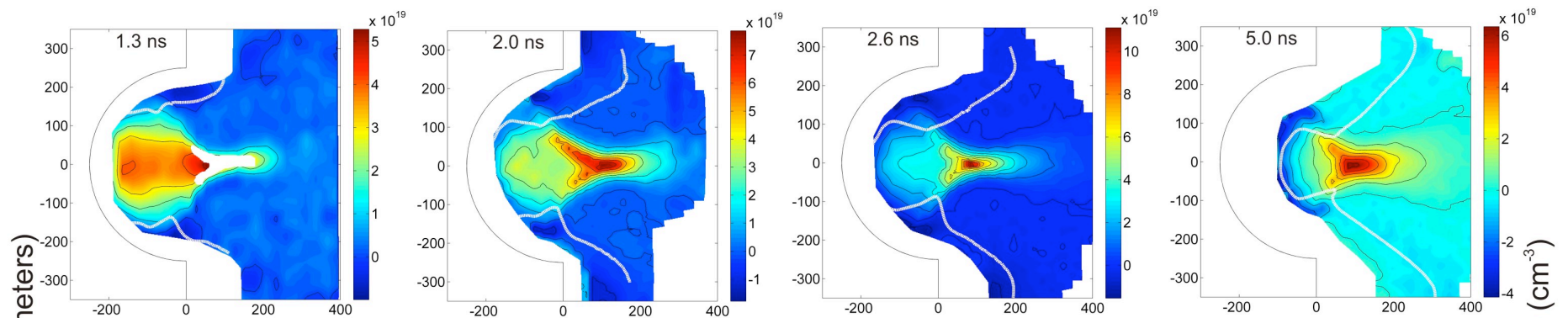
**Carbon plasma converging plasma forms early ~1 ns
and is still visible at late times ~17 ns**



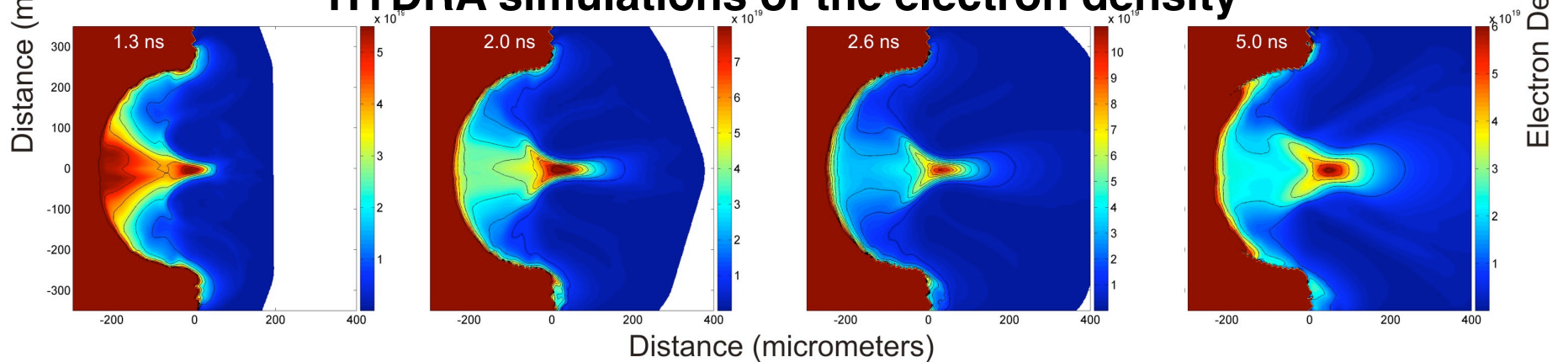
Comparison with HYDRA show excellent agreement in area where free electron contribution to fringes dominates



Electron density maps obtained with the SXR interferometry



HYDRA simulations of the electron density



J. Filevich, J.J. Rocca, M.C. Marconi, S.J. Moon, J. Nilsen, J.H. Scofield, J. Dunn, R.F. Smith, R. Keenan, J.R. Hunter, V.N. Shlyaptsev, "Observation of a multiply ionized plasma with index of refraction greater than one", Phys. Rev. Lett. 94, 035005, (2005).

Excellent agreement with code result from high collisionality of plasma under these conditions

Ion-ion collision frequency including the relative drift velocity $[\Delta v]$

$$\nu_{\alpha\beta} = \frac{8\sqrt{\pi} Z_{\alpha}^2 Z_{\beta}^2 n_{\beta} \Lambda}{m_{\alpha\beta}^2 (\Delta v)^3} \left[\frac{\sqrt{\pi}}{2} \operatorname{erf}\left(\frac{\Delta v}{v_{th}}\right) - \left(\frac{\Delta v}{v_{th}}\right) \exp\left(-\frac{\Delta v^2}{v_{th}^2}\right) \right]$$

$$\Delta v = |\mathbf{v}_{\alpha} - \mathbf{v}_{\beta}| = 2|\mathbf{v}_{\alpha}| \sin\left(\frac{\theta}{2}\right)$$

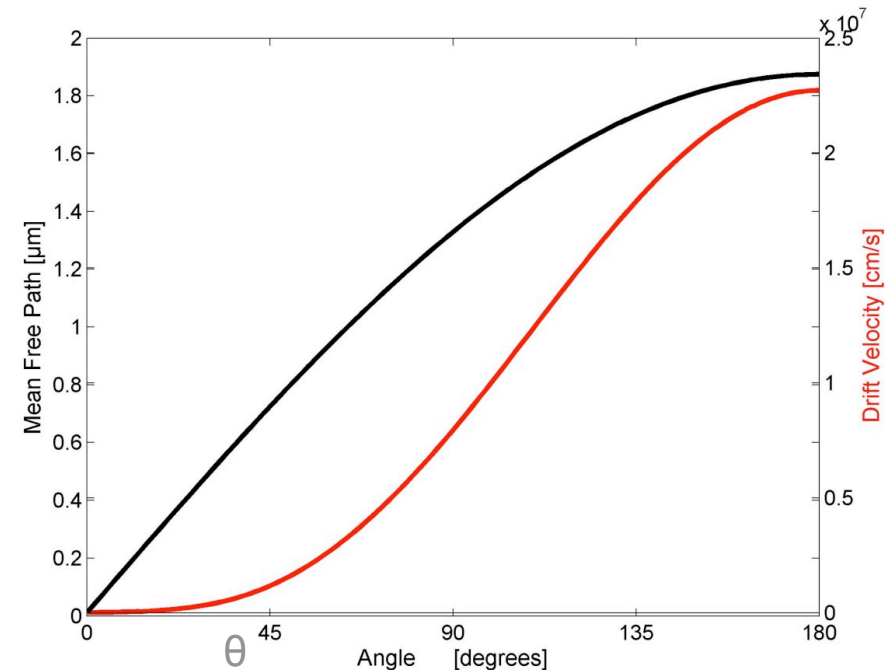
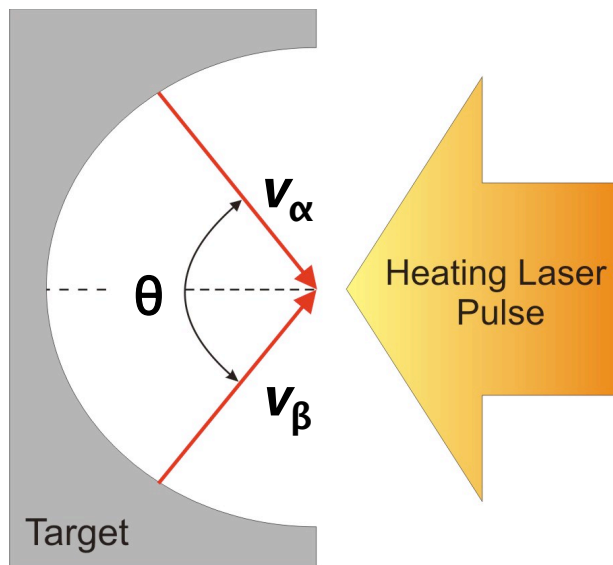
Carbon:

$$N_e = 1 \times 10^{20} \text{ cm}^{-3}$$

$$T_e \approx T_{ion} = 50 \text{ eV}$$

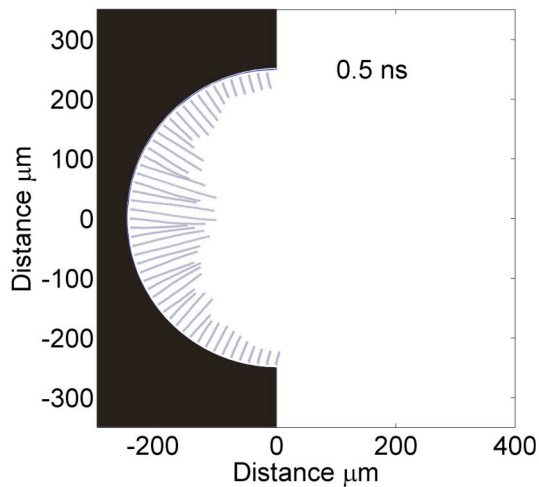
$$Z_{\text{mean}} = 5$$

David Larsen (LLNL)

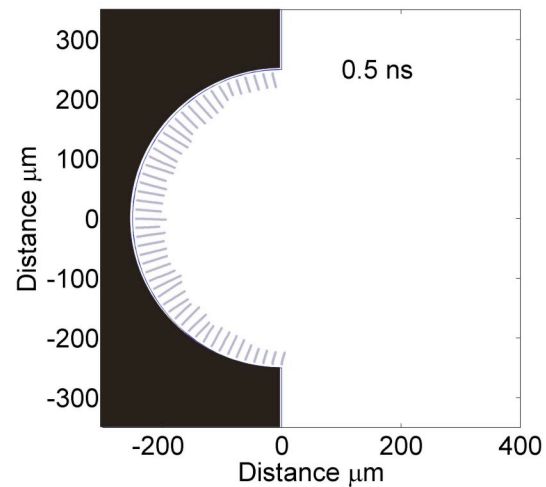
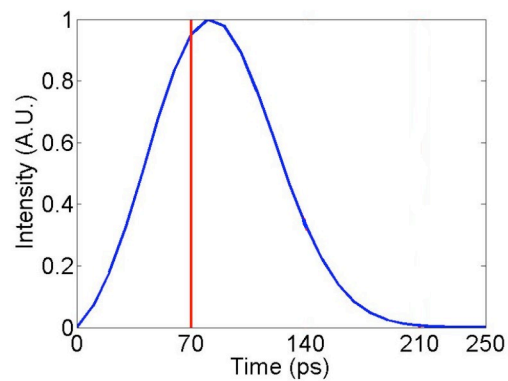


Maximum mean free path $< 2 \mu\text{m}$ indicates highly collisional regime

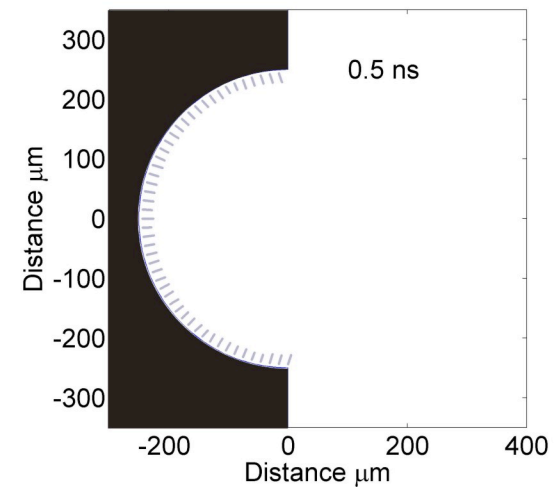
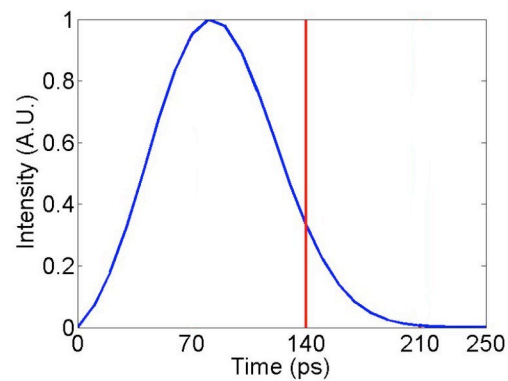
Tracer particle analysis of colliding plasma shows role of different cylinder areas



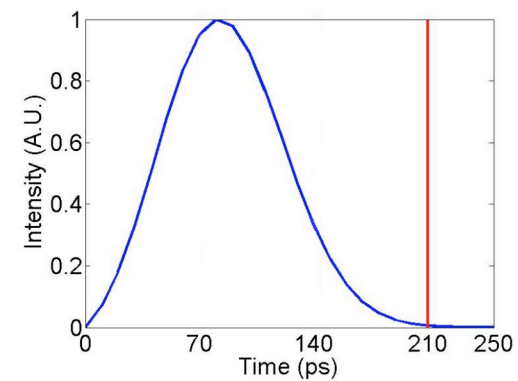
70 ps



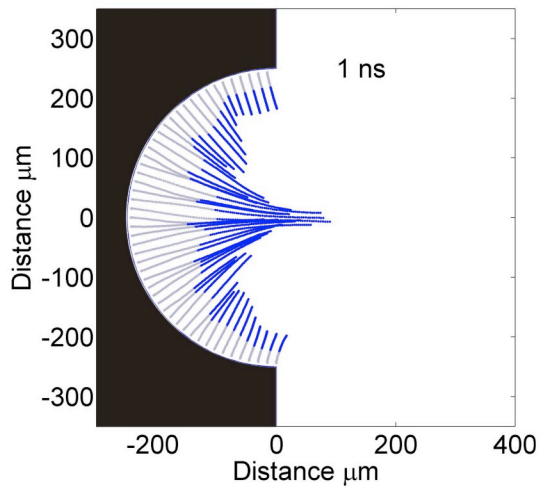
140 ps



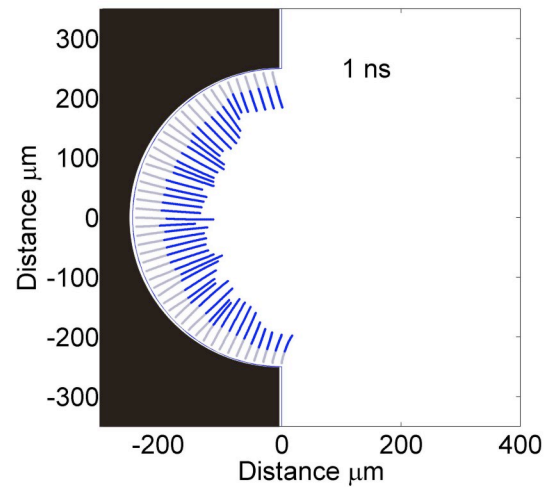
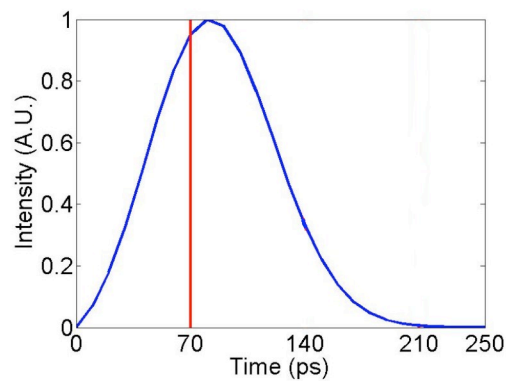
210 ps



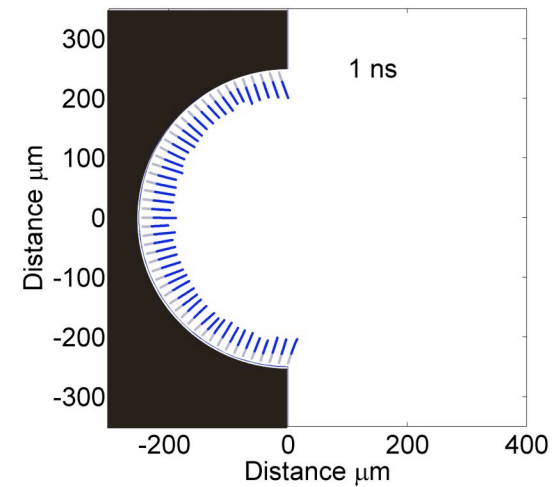
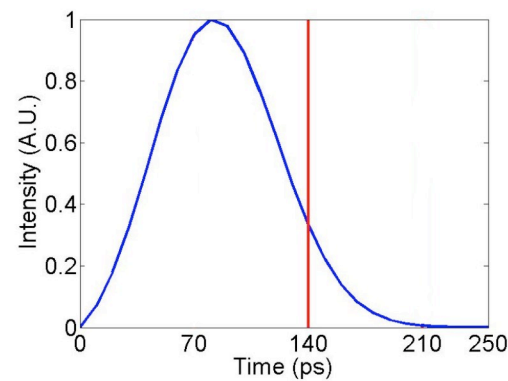
Tracer particle analysis of colliding plasma shows role of different cylinder areas



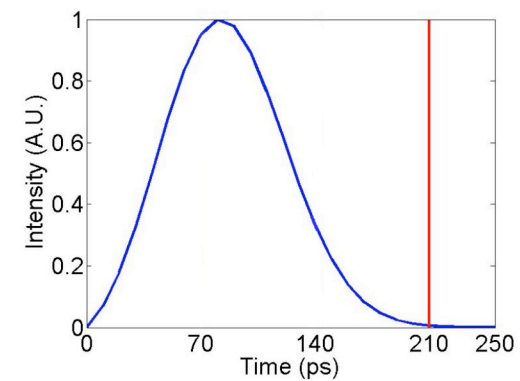
70 ps



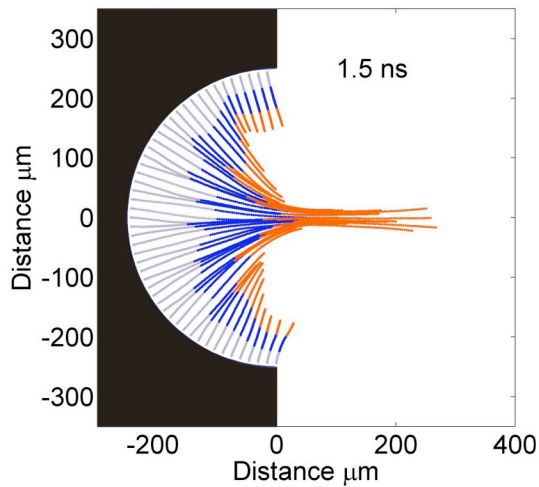
140 ps



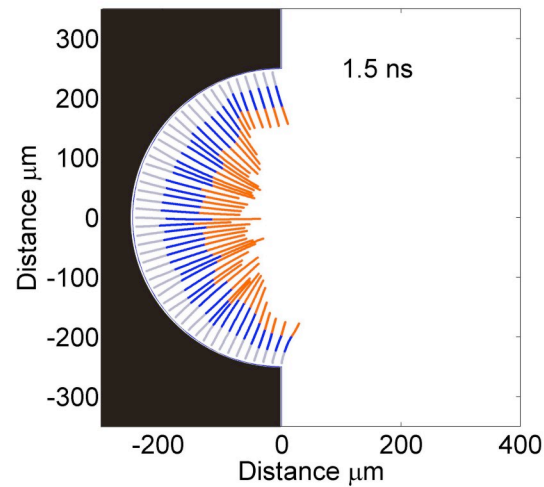
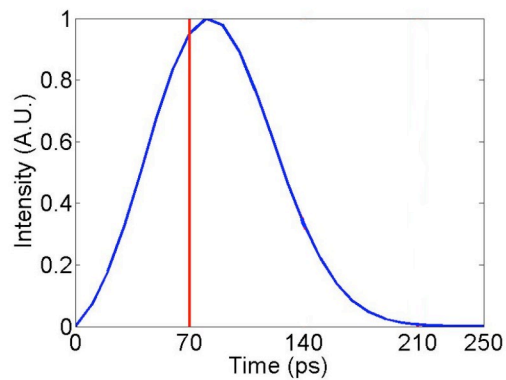
210 ps



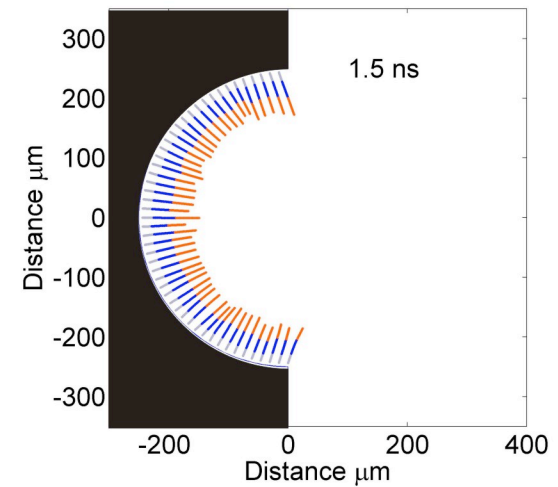
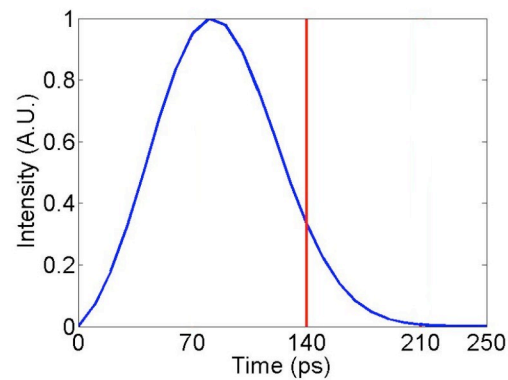
Tracer particle analysis of colliding plasma shows role of different cylinder areas



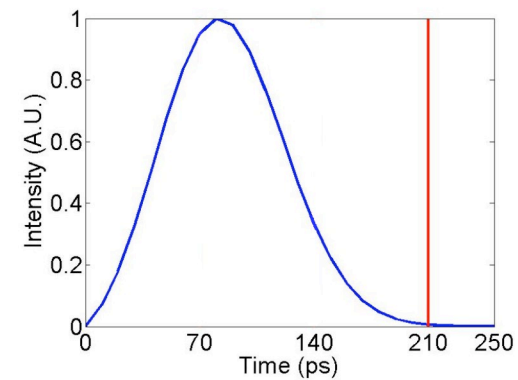
70 ps



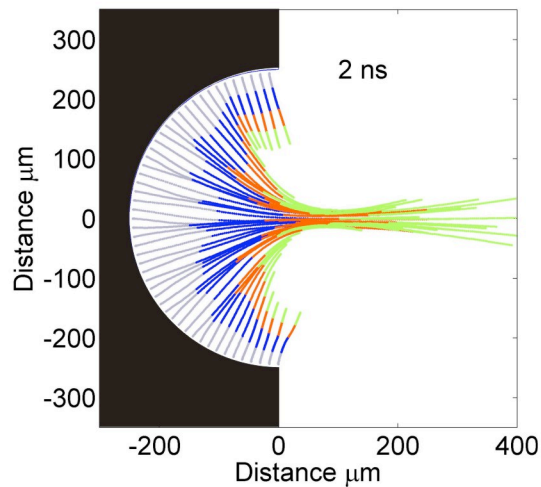
140 ps



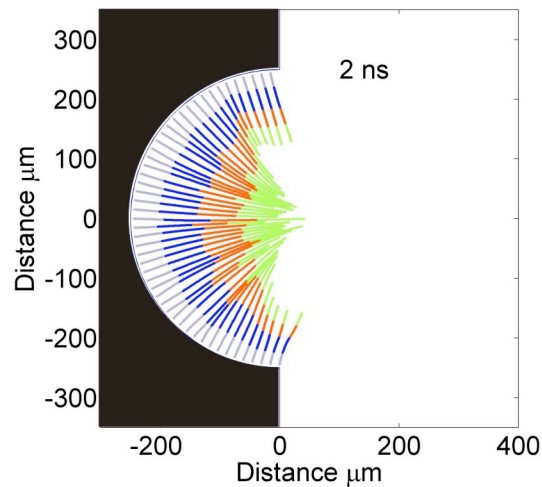
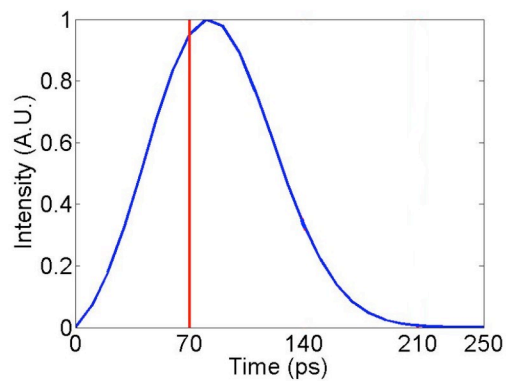
210 ps



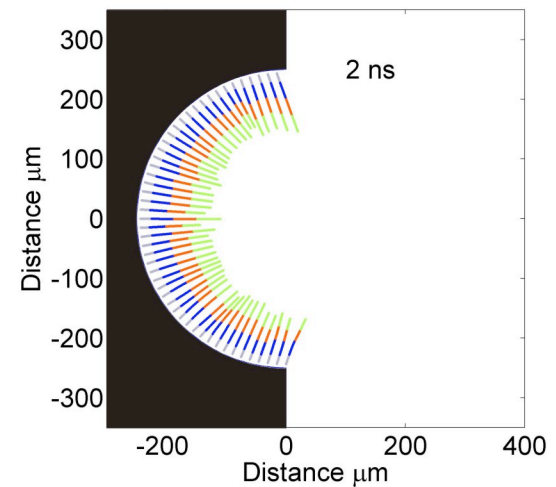
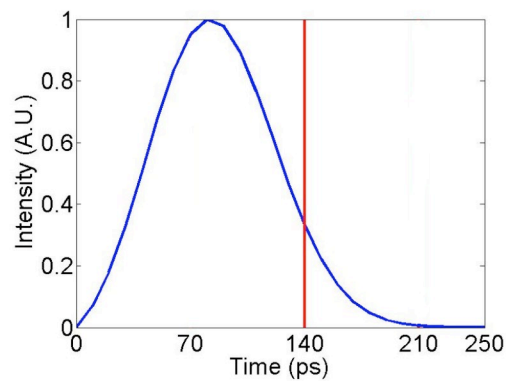
Tracer particle analysis of colliding plasma shows role of different cylinder areas



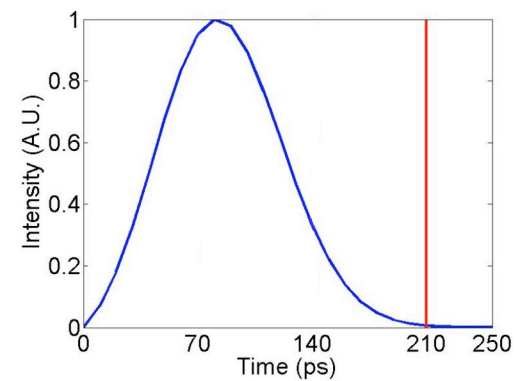
70 ps



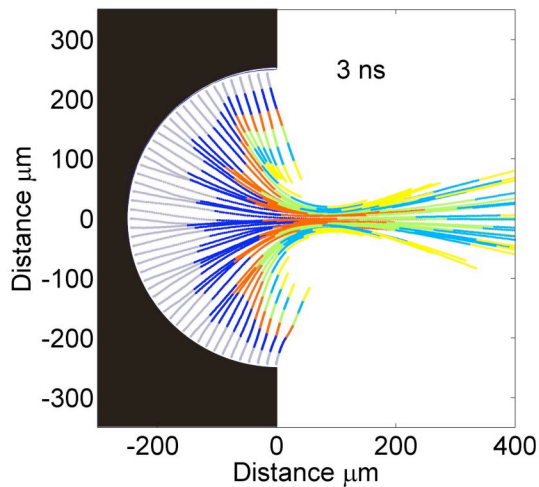
140 ps



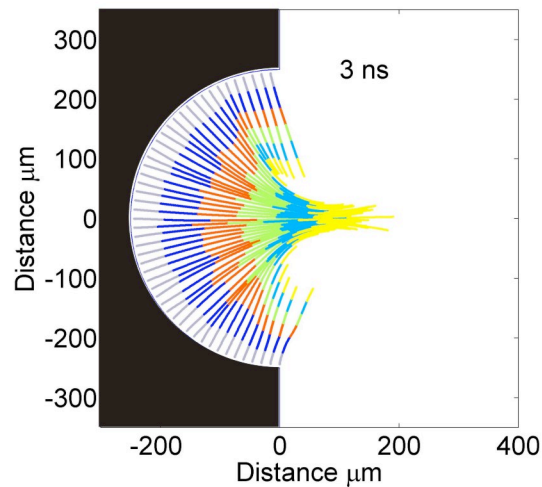
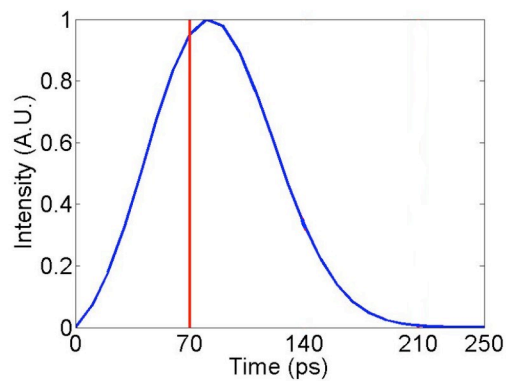
210 ps



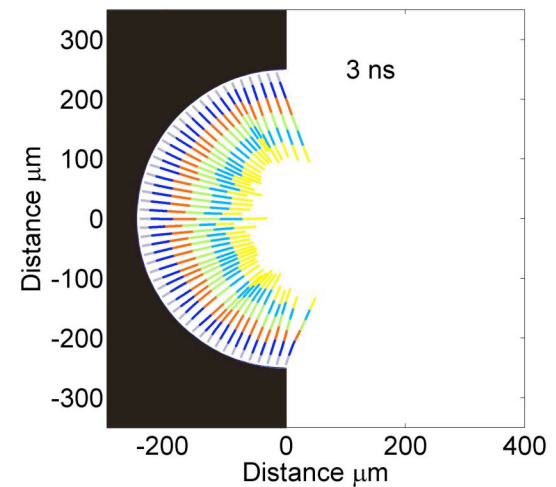
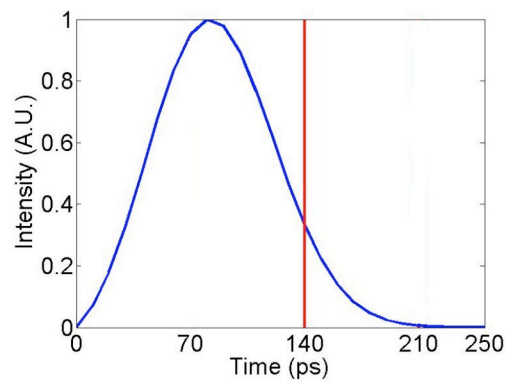
Tracer particle analysis of colliding plasma shows role of different cylinder areas



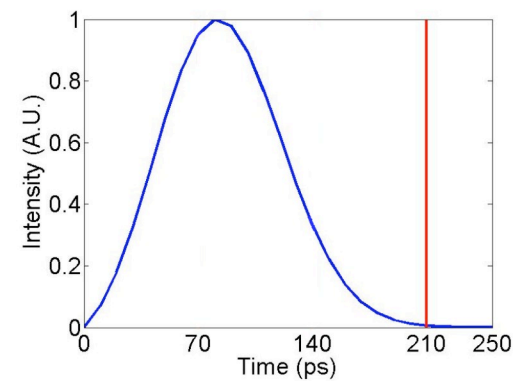
70 ps



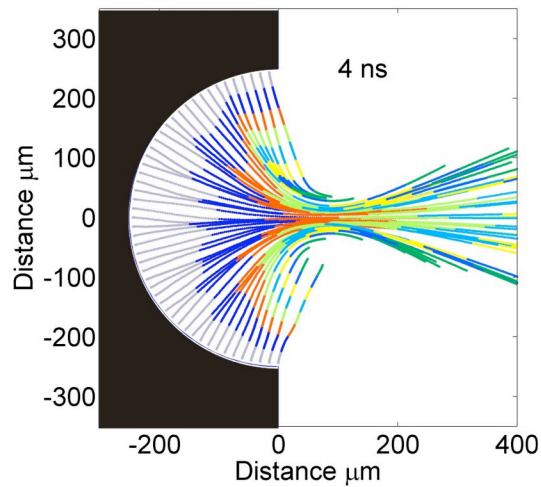
140 ps



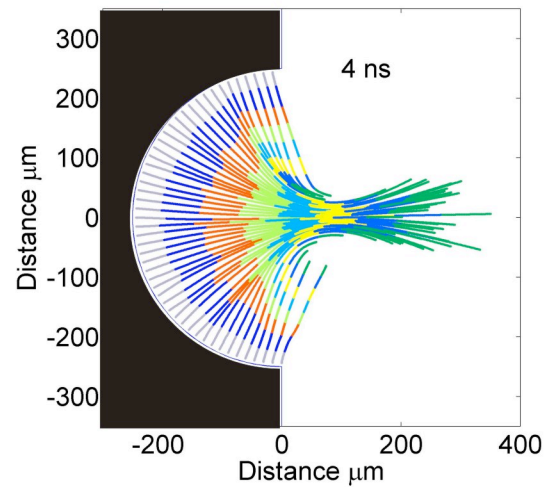
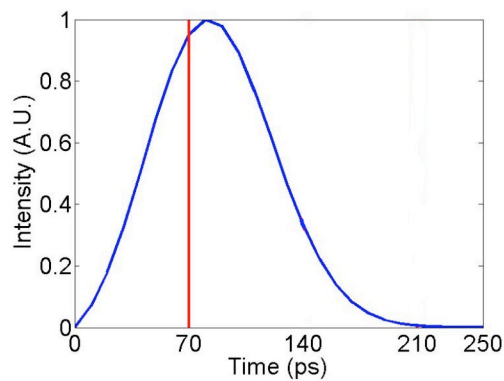
210 ps



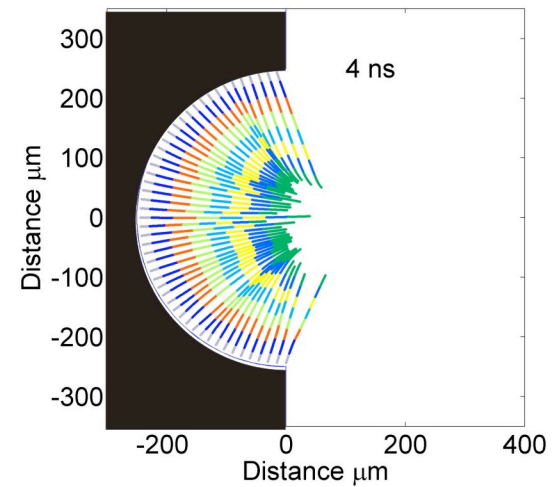
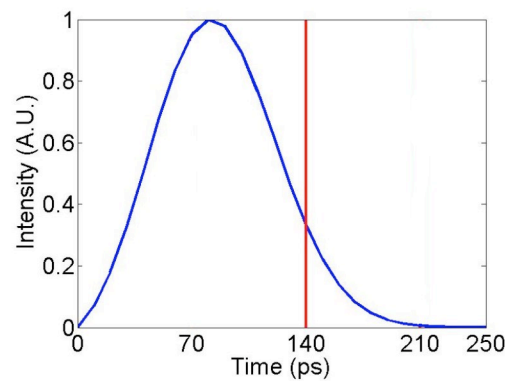
Tracer particle analysis of colliding plasma shows role of different cylinder areas



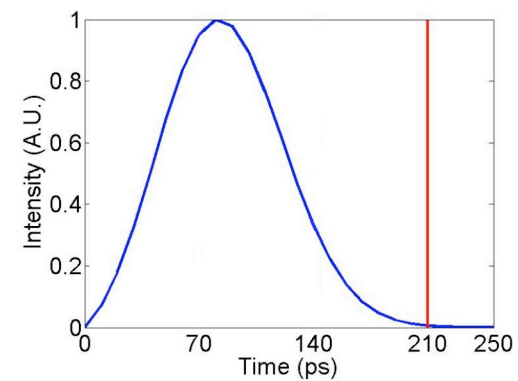
70 ps



140 ps



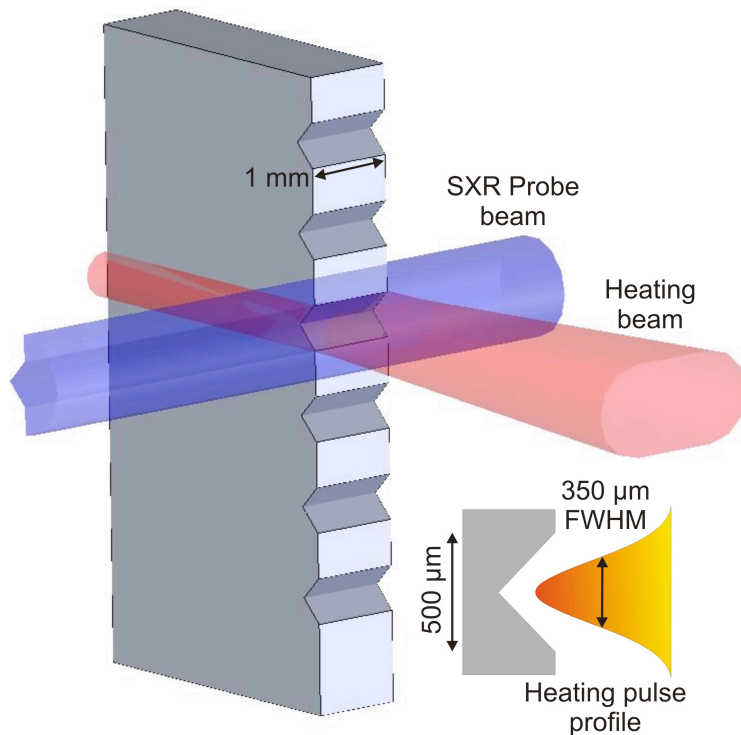
210 ps



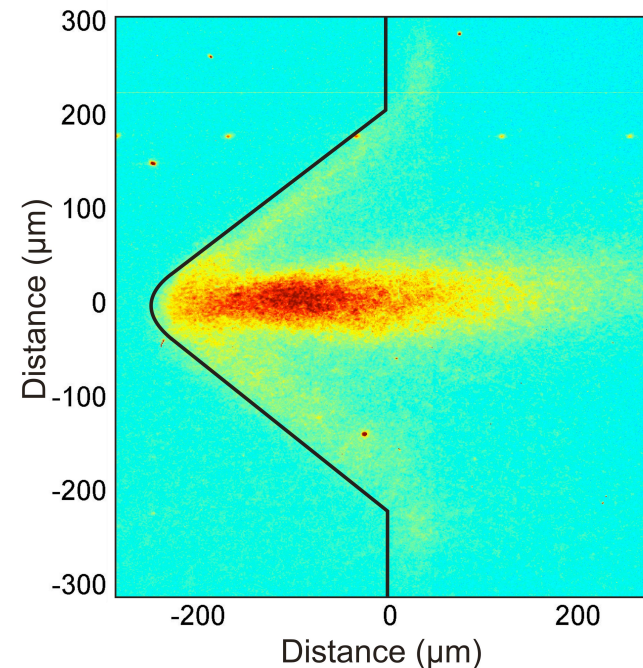
IV. V-groove targets produce planar colliding plasmas for study: Collimated jet structures are observed

Laser Irradiation conditions:

- $1.2 \times 10^{12} \text{ Wcm}^{-2}$, 800 mJ at 800 nm wavelength, 120 ps (FWHM)
- Laser focus: $350 \mu\text{m} \times 1.5 \text{ mm}$ line
- Targets: Al $500 \mu\text{m} \times 1 \text{ mm}$ wide



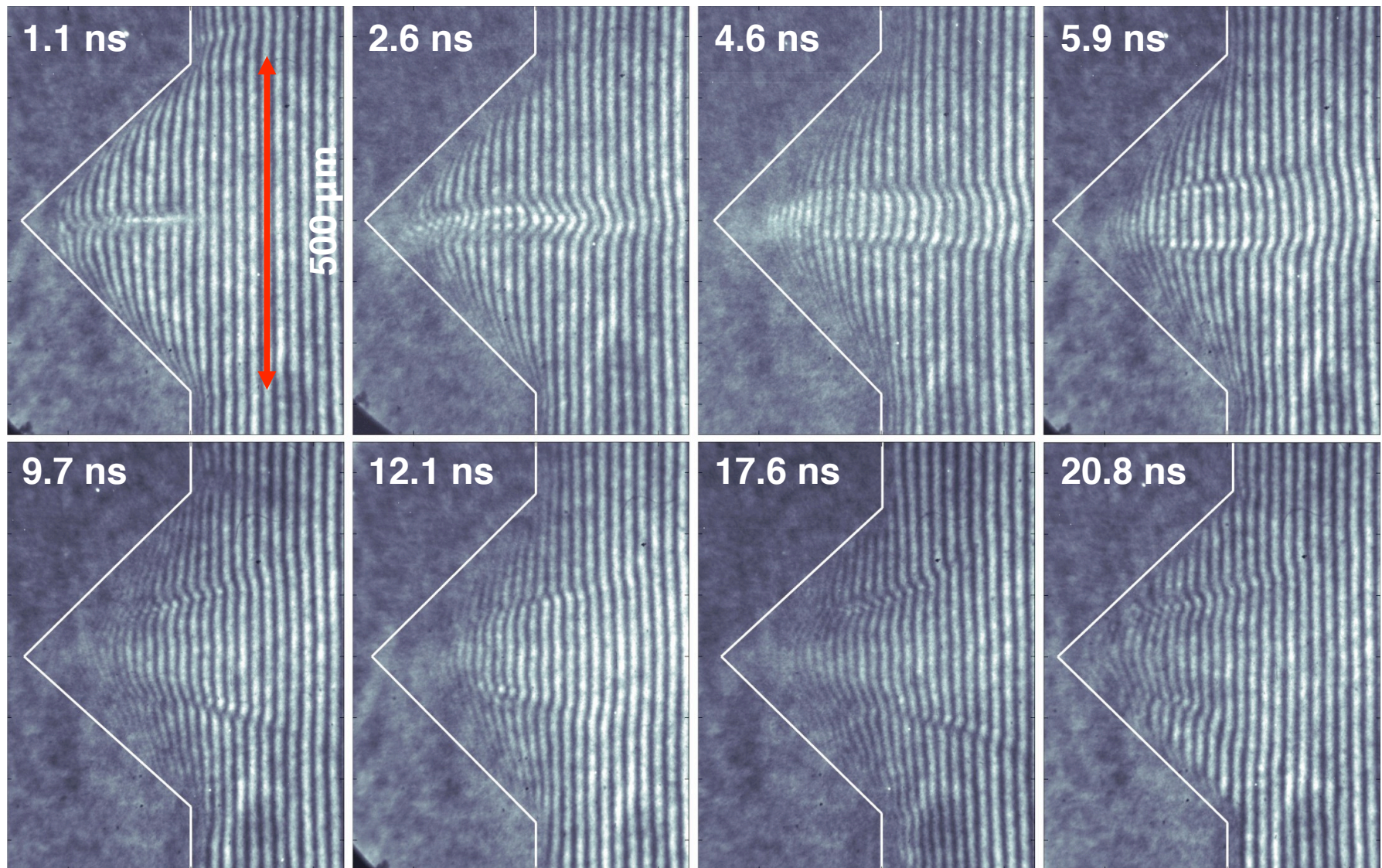
Time-integrated soft x-ray self-emission viewed on axis



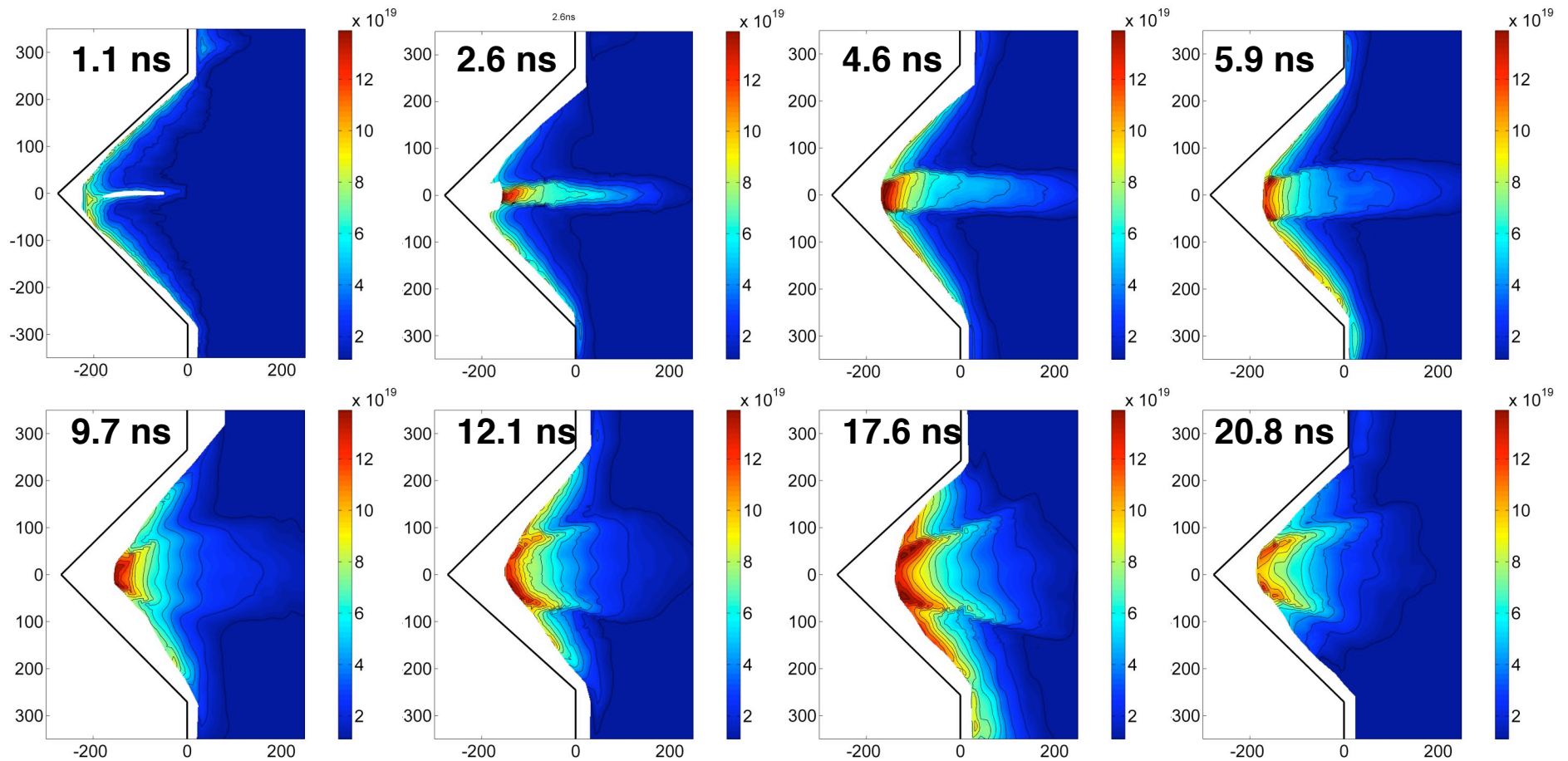
J. Grava, M.A. Purvis, J. Filevich, M.C. Marconi, J.J. Rocca, J. Dunn, S.J. Moon, and V.N. Shlyaptsev, *Phys. Rev. E* **78**, 016403, (2008).

Soft x-ray emission shows strong collisional heating of plasma on-axis

Jet like structure forms in Al colliding plasma very early in time and remains collimated until after 6 ns

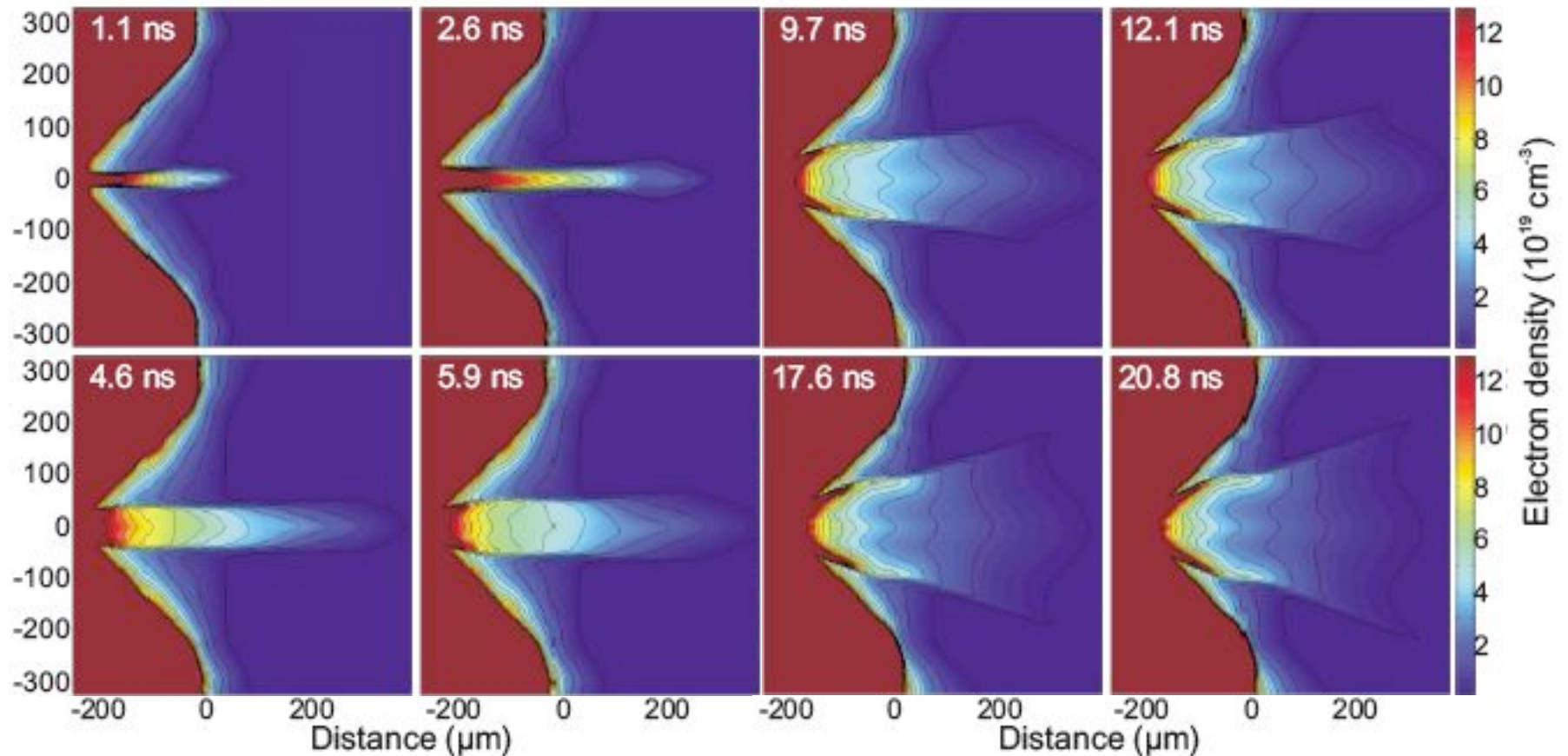


Density maps show jet loses collimation and lobe structures form at periphery at late times

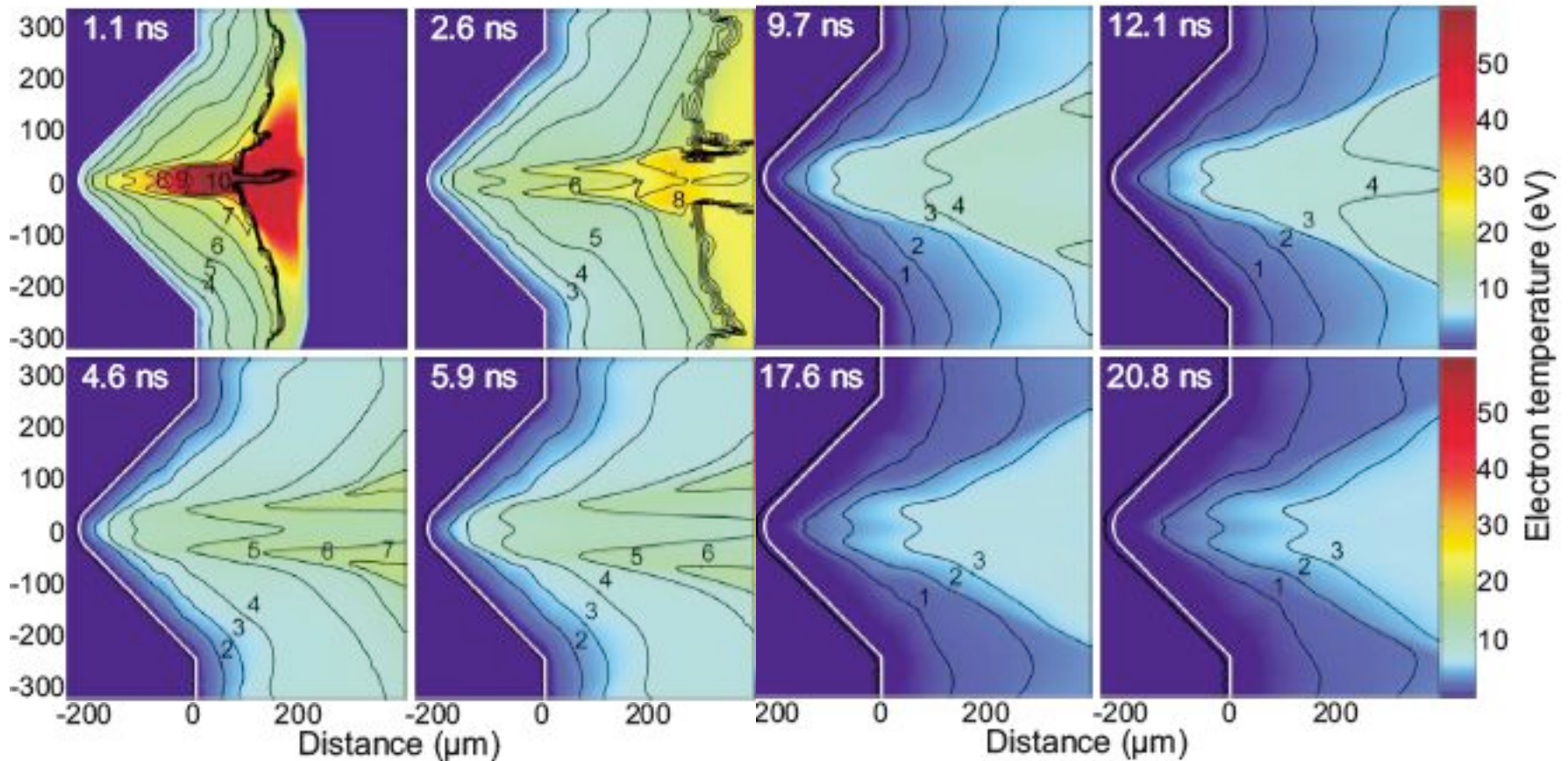


Micrometers

2-D HYDRA simulations are in excellent agreement with data showing evolution of main features

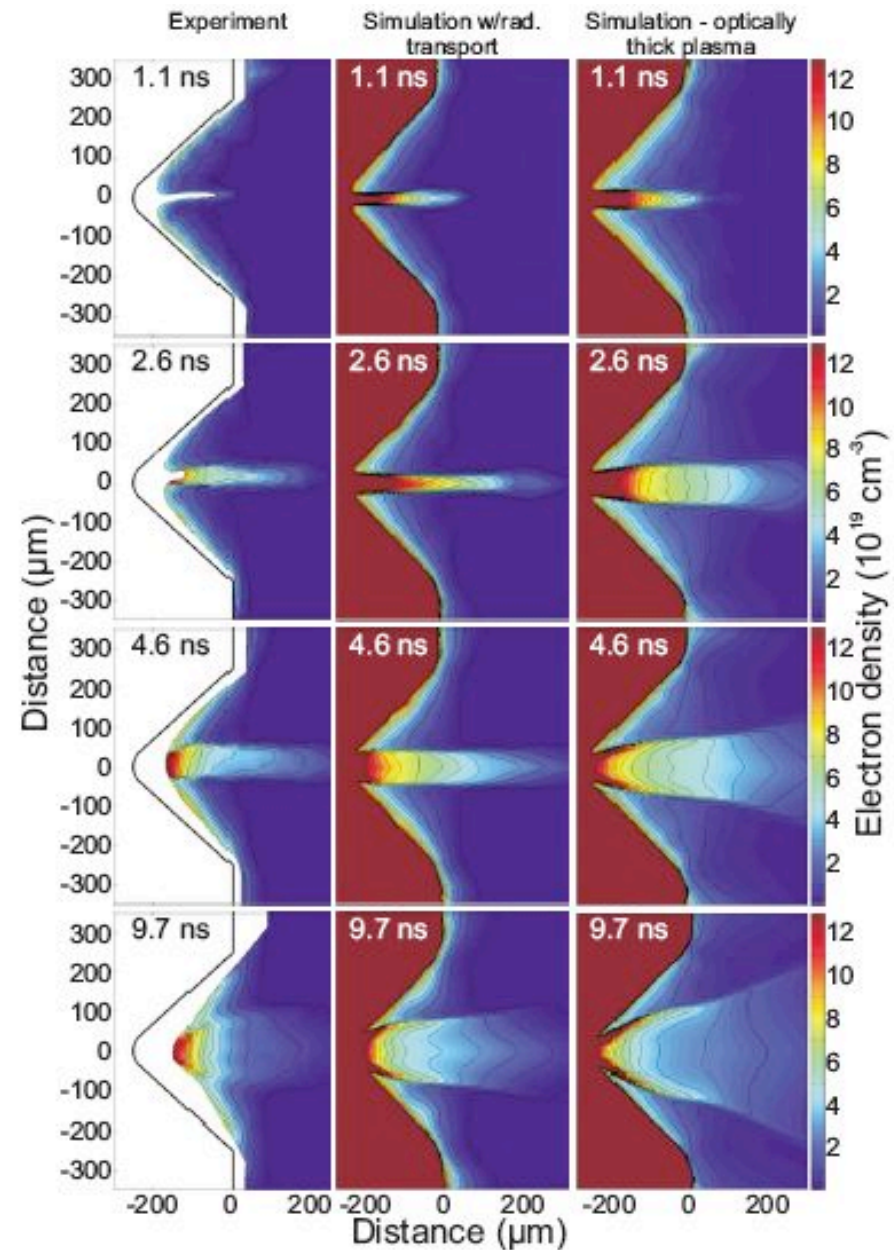
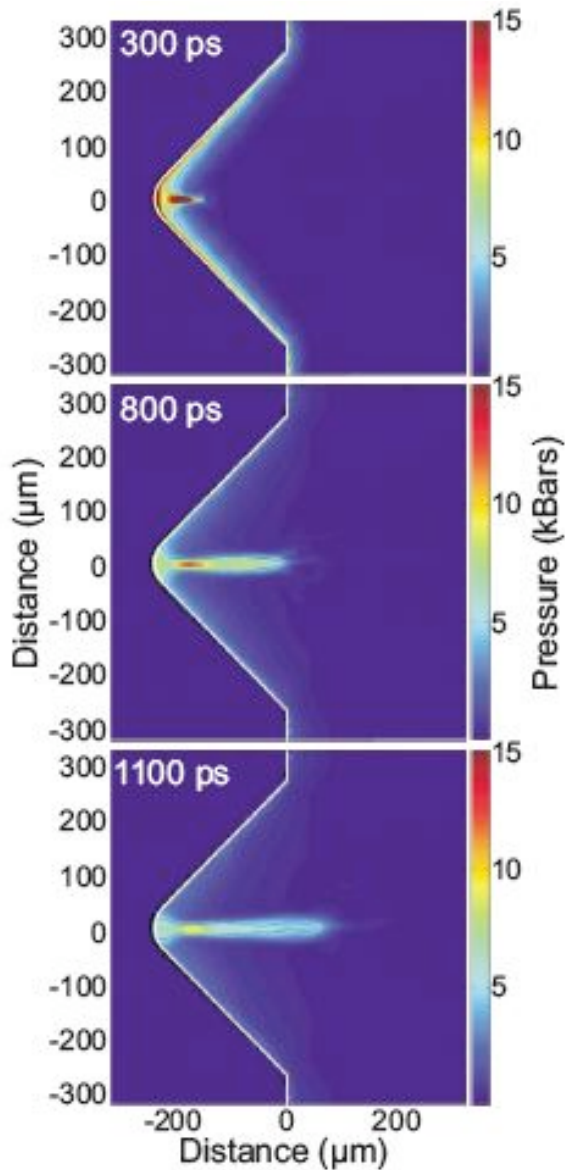


2-D HYDRA simulations show temperature and ionization of the colliding plasma at various times



J. Grava, M.A. Purvis, J. Filevich, M.C. Marconi, J.J. Rocca, J. Dunn, S.J. Moon, and V.N. Shlyaptsev, Phys. Rev. E 78, 016403, (2008).

Optical thickness and radiation transport in plasma jet affects collimation at all times



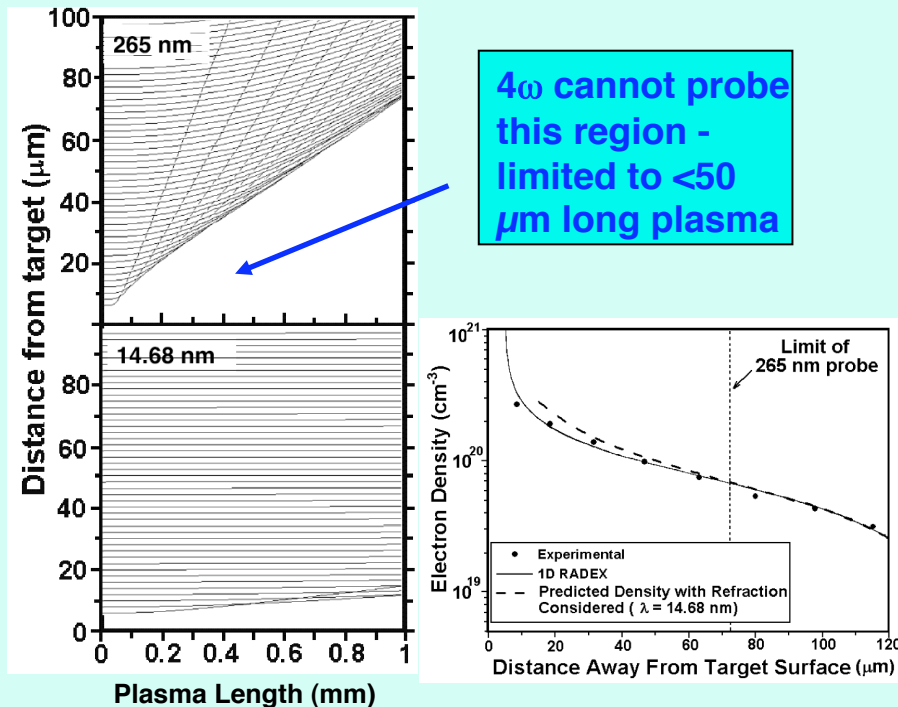
Summary



- **Soft x-ray laser interferometry is a powerful diagnostic for studying the evolution and physics of dense, confined plasmas**
- **2-D Density profile of colliding plasmas for semi-cylindrical and V-targets have been measured and compared with 2-D HYDRA simulations**
- **Aluminum and Carbon Half-hohlraum targets:**
 - Comparison with HYDRA simulations in excellent agreement (highly collisional)
 - Density peak exceeding 10^{20}cm^{-3} measured near or slightly outside axis
 - For Carbon: code simulations for plasma Zbar help to determine regions of plasma where free electron approximation is valid
 - Plasma build-up is mainly the result of convergence of plasma (perpendicular from surface) towards the axis of the cavity (late time contributions from wall)
- **V groove targets:**
 - Open target design allows observation of colliding plasma away from wall
 - Observed early density build up on axis creates a jet
 - Degree of collimation of jet determined by balance of external pressure and internal temperature of jet
- **Detailed testing of code physics allows simulations of groove targets where plasma confinement and proximity heating of walls are extreme**

Ray-tracing shows reduced refraction with 14.7 nm probe allows probing closer to target surface

Refraction of 4ω vs 14.7 nm of 1 mm Al plasma with shown density profile



4ω cannot probe this region - limited to $<50 \mu\text{m}$ long plasma

Al plasma, XRL at $\Delta t = 700 \text{ ps}$ R. Smith *et al.*, JOSA B 20, 254 (2003).

Technical Advantages of X-ray Laser Interferometry

- 2 - 5 ps pulse duration measured
 - $T_e \sim 100 \text{ eV}$, $v_s \sim 5 \times 10^6 \text{ cm/s}$
 - $\Delta x \sim 0.25 \mu\text{m}$, minimal plasma motion
- Short wavelength 14.7 nm
 - Sub-micron spatial imaging
 - Reduced plasma absorption e.g. free-free abs. ($\sim \lambda^3 [1 - \exp(-hc/\lambda kT)]$)
 - Reduced plasma refraction ($\theta \sim \lambda^2$)
 - 4ω probe requires *a priori* knowledge of plasma density to remove refraction
- Multilayer optics, gratings available for instrumentation
- Can be scaled to shorter wavelengths and Petawatt pumping for NIF experiments including hohlraums

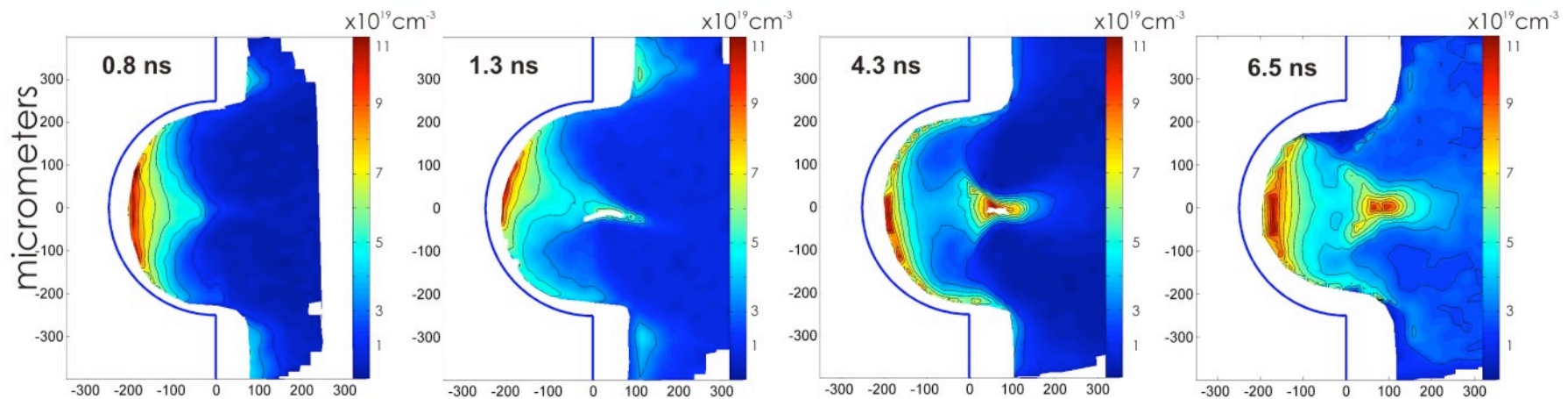
X-ray laser interferometry combined with ps duration allows study of various LPP energy transport mechanisms at target surface

Aluminum target comparison for electron density maps with HYDRA simulations



Laser Irradiation: 10^{12} Wcm^{-2} , 600 mJ at 800 nm, 120 ps (FWHM), $300\mu\text{m} \times 1.5\text{mm}$ line focus

Electron density maps obtained with the SXR interferometer



HYDRA simulations of electron density maps

